Imaging Characteristics of Typical and Atypical Ovarian Teratoma, Comprehensive Review: Radiologic Pathologic Correlation

SAFIA BADR SAYED, M.D.¹; HODA MAGDY ABBAS, M.D.²; AALAA SOBHI ABDELGHANI, M.D.³; RADWA ESSAM MOSTAFA, M.D.⁴ and AHMED E. HASSAN, M.D.⁵

The Department of Radiology, Faculty of Medicine, Cairo University and Radiology Department, National Cancer Institute, Faculty of Medicine, Cairo University,

Abstract

Background: Germ cell tumors that make up about 20% of all ovarian tumors are called ovarian teratomas, their most common types are typical and atypical ones. Because of the unique intratumoral fat component, they are usually easily detected by imaging techniques. Various unusual imaging findings, on the other hand, can be highly deceiving.

Aim of Study: This study highlighted the role of Ultrasonography (US), Computed Tomography (CT) and Magnetic resonance imaging (MRI) in identification of atypical mature ovarian cystic teratomas depending on its components or complications in female patients for better prognosis and early successful management.

Patients and Methods: In this cross-sectional analytic study, eighty female patients underwent the US. CT was done in ten cases, MRI in fifteen cases, and five cases were subjected to both CT & MRI. Their ages ranged from 13-50 years.

Results: In our study, fifty cases were diagnosed as typical teratoma and thirty cases were atypical. Histopathological correlation was done for all participants. The sensitivity of US was 100% in the detection of typical Mature cystic teratoma (MCT) without the need for other imaging modalities. While in atypical cases, the US wasn't conclusive. The added imaging tools of MRI and CT in the US raised the sensitivity for the diagnosis of atypical cases up to 86.6%.

Conclusions: Ultrasound is the primary imaging modality. In typical cases; no further imaging will be required. US combined with CT/MRI can detect properly atypical imaging findings of ovarian teratomas. CT alone was excellent in macroscopic fat and calcification detection, and MRI was superior in microscopic fat detection and was an adjuvant tool in keratin identification by the modality of DWI, especially in fatless MCT.

Correspondence to: Dr. Safia Badr Sayed, The Department of Radiology, Faculty of Medicine, Cairo University

Key Words: MRI – CT – US – Ovarian teratoma – Typical – Atypical features.

Introduction

THE most prevalent ovarian germ cell tumor is a teratoma. Due to their diverse germ-cell origins, these tumors are pluripotent. It is accounting for 20% of adult ovarian tumors and 50% of pediatric ovarian tumors [1]. The most prevalent subtype of ovarian teratomas, mature teratomas, commonly referred to as dermoid cysts, account for 69% of all germ cell tumors and over 95% of all teratomas. Ten percent of GCT are immature teratomas, the second most prevalent subtype of teratomas [3].

Ovarian teratomas can develop in a variety of ways, from tiny masses discovered by chance to malignantly altered tumors with a high mortality rate. Although the most common ovarian teratoma imaging results are the intratumoral fat, various atypical features also can be detected ranging from purely cystic to a firm solid mass. These atypical manifestations are depending on tumor components or complications, in which variable intermixed histologic tissues result from a common stem cell [2].

Understanding the atypical manifestations of the MCTs is very critical and important for better

List of Abbreviations:

CT : Computed tomography.

DWI: Diffusion-weighted imaging.

US: Ultrasonography.

MCT : Mature cystic teratoma. MR : Magnetic resonance.

MT : Mature teratoma.

SCC : Squamous cell carcinoma. DWI : Diffusion weighted imaging.

ADC: Apparent adhesion coefficient.

prognosis and early management application of the patients. Since it can be challenging to distinguish ovarian teratomas from other epithelial neoplasms, a small fraction of them may be missed in the few tumors that do not contain fat. Additionally, it is essential to understand the imaging results of MCT problems since prompt and precise diagnosis of these issues is critical to providing the best possible care for patients and averting disastrous health outcomes [9].

A cystic mass with a densely echogenic tubercle (Rokitansky nodule) extending into the cystic lumen or a diffusely or partially echogenic mass exhibiting sebaceous material and multiple thin echogenic bands due to hair in the cyst cavity are the most commonly observed imaging features of teratomas in the United States. Intratumoral fat showed attenuation on CT. Intrathemoral fat was found using MR imaging with T1-weighted imaging and fat-saturated T1-weighted imaging.

Calcification is common in addition to intratumoral fat, however finding intratumoral fat is critical for confirming the diagnosis [6].

CT was mainly highlighted in earlier diagnosis of the unusual manifestation of MCTs depending on its complication especially torsion and rupture due to its lower cost and its availability than MRI.

Also its superiority in better and easier bone density/calcification identification. Sometimes it contributed in diagnosis of the presence of the intralesional keratinoid substance which displayed hypoattenuation of the spheroids averaged between –2 HU and 0 HU. Bernot et al., 2017

MRI has played crucial role in identification of both macro/microscopic fats. The cystic wall of the

MCTs must be carefully examined to do the correct preoperative diagnosis. To show microscopic fat on MR images, a gradient-echo technique with both in-phase and opposed-phase imaging is very useful. This technique is probably superior to the use of fat saturation method. S. Wakrim 2020.

DWI has played an important role in identification and understanding the atypical MCTs especially in cystic or complex cystic ovarian lesions. As high signal of DWI and the calculated low ADC values distinctly identify the keratinoid substance of MCTs which displayed water density and signal on both CT and conventional MRI sequences. Tomohiro Nakayama 2005.

The goal of this study was to use multiple imaging modalities (US, CT, and MRI) to determine the typical and atypical features of teratomas with the

concern of complications. Understanding the unusual imaging features of mature cystic teratomas allows for a more precise diagnosis.

Patients and Methods

This retrospective study was performed between January 2021 and February 2022 and was approved by our Research and Ethical Committee.

Study group:

This study was conducted on 80 female patients, ages ranging from 13-50 years. They were referred to the radiology department for an assessment of their complaint.

Inclusion criteria:

- Patients with a clinical complaint of abdominal, and pelvic pain suspected to be adnexal in origin.
- 2- Patients were found to have adnexal masses on their ultrasound examination on their regular checkup or as routine examinations for job qualifications even there were asymptomatic.

Exclusion criteria:

- 1- CT in Pregnant females.
- 2- Incomplete full radiological results to reach the final diagnosis in comparison with histopathology.

All patients were subjected to the following:

- 1- A thorough examination of their problems, relevant past medical and surgical history, General, abdominal, and pelvic physical examination, and revision of previous imaging studies (if available).
- 2- Tumor markers; (CA 125, CA 19-9, B HCG, and AFP) if available.
- 3- Two experts with at least ten years of gynecological ultrasonography experience performed the US examination. (General Electric, Voluson Pro 700, New York City, USA). Either a transabdominal probe operating at 5.0–7.0 MHz and/or a 3.5-7.5 transvaginal probe were used. We classified the data collected from examined patients into typical (n=50) and atypical groups (n=30) based on the preliminary US findings.
- 4- For atypical group demonstrated in our study by the US, those patients were subjected to further imaging modalities for accurate diagnosis. Ten cases underwent CT, fifteen underwent MRI, and five underwent both CT/MRI.
- 5- The specific requirements for CT acquisition with a 32-channel multi-detector CT scanner (GE) were as follows: Standard tube current

(60–120 mAs) and tube voltage (120–160 kVp). Slice thickness of 3.0mm reconstruction interval of 1.0–3.0mm. Both oral and IV contrast was used only in predominant solid or complex ovarian lesions. Oral contrast aided to differentiate cystic adnexal lesions from the bowel.

- 6- A Siemens MAGNETOM Avanto 1.5 T machine with a 60cm bore size, 160cm system length, and Zero Helium boil-off technology was used to perform the MRI. Axial images were produced using a 256 x 256 matrix, a 32cm field of view, and a 4mm slice thickness. Brief T1 inversion recovery (STIR), transverse T2-weighted, transverse T1-weighted, and turbo spin-echo sagittal. In and out phases of axial T1. Prior to and following intravenous gadolinium infusion (0.2mL/kg (0.1mmol/kg) at a rate of 10mL per 15 seconds), fat-suppressed T1W sequences were also acquired. At a low b value of 0, diffusion-weighted imaging (DWI) was performed and high b values > b800. Apparent diffusion coefficient (ADC) maps were calculated. The cutoff ADC value of malignancy was $1.2 \times 10^{-}$ mm⁻/s.
- 7- All radiologically diagnosed ovarian teratomas in both study groups were correlated to postoperative histopathological results.

A: Imaging interpretation of Typical group:

During the inspection of the typical group cases (n=50) based on their US findings, all patients' US examinations showed the typical US characteristics for MCTs diagnosis without any further needed radiological tool (Table 1). Teratomas 5–6cm in premenopausal patients were evaluated for surgical resection (cystectomy). However, because of the increased documented risk of torsion and malignant transformation, oophorectomy was the preferred treatment for resection in postmenopausal women, even when it was smaller. Postoperative histopathological assessments were performed and correlated with our radiological data.

B: Imaging interpretation of Atypical group:

Those cases showed atypical findings based on their US studies and needed more radiological tools aiding to reach their final diagnosis. The US results of those cases were represented by the followings:

- Purely Cystic lesion with a scanty amount or without intracystic fat.
- 2- Purely fatty lesion.
- 3- An ovarian lesion that was mostly solid and diverse, with few fatty regions.
- 4- Two septated cystic masses, one of which contains intratumoral fat and the other of which is

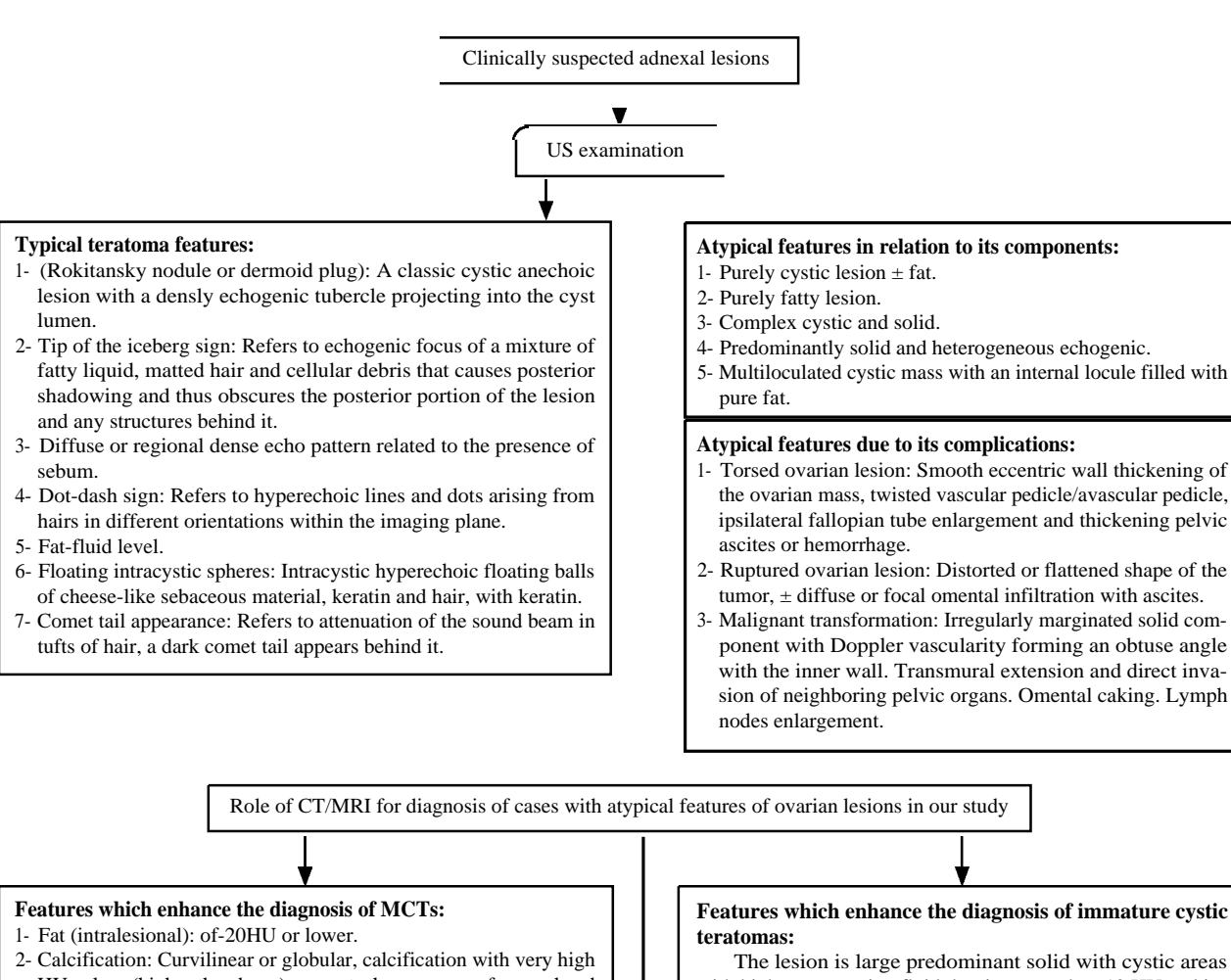
- multiloculated cystic in nature, were located close to each other.
- 5- Multiple cystic and solid areas with a complex appearance.
- 6- The presence of ascites and a distorted or flattened shape of an ovarian lesion with a discontinued wall.
- 7- Color Doppler shows a cystic, solid, or complicated mass with or without pelvic fluid, wall thickening, and cystic hemorrhage with twisted vascular pedicle ("whirlpool sign") or avascular pedicle.

In those group either CT, MRI, or both were done. The choice decision of CT/MRI was dependent on the US appearance and clinical data of the patients. The added value of CT in our study was notably appeared in complicated ovarian masses with acute abdominal pain, the presence of primitive voluminous ascites, and ovarian lesions with calcification/bone density. In addition to delineating the effect of the mass on surrounding structures and preoperative staging if malignancy was suspected.

While the role of MRI was clearly evident in soft tissue characterization of solid-containing ovarian lesions. It also can demonstrate the microscopic fat by using T1 in and out phases, DWI has an important role in the detection of keratin especially when the amount of fat was very scanty, and also helping to expect and diagnose malignant transformation of the underlying teratoma.

In our included atypical group cases, their management were done depends on the tumor's grade; less severe tumors can be treated with surgery alone, but more advanced cancers typically need both surgery and chemotherapy. Only surgical resection is used to treat benign struma ovarii tumors. On the other hand, surgical removal of malignant struma ovarii is followed by adjuvant treatment, such as radioiodine ablation therapy and/or thyroxine supplementation. Surgery, either with or without adjuvant chemotherapy, was used to treat additional monodermal teratomas, including neuroendocrine tumors and neuroectodermal tumors.

We arranged our steps for an accurate diagnosis of MCT based on different imaging modalities for both typical and atypical findings in an algorithmic way for easier identification of MCT based on many previous studies of literature [L. Saba et al., Rha et al., Hilal Sahin et al., and Mohammed Saleh et al.]. The presence of calcification and fat independent of its amount should raise our suggestive possibilities for MCT diagnosis Fig. (1).



- 2- Calcification: Curvilinear or globular, calcification with very high HU values (higher than bone) suggests the presence of enamel and a tooth-like structure.
- 3- Fat-fluid level/floating nodule.
- 4- Hair tuft.
- 5- Floating balls sign.
- 6- Macroscopic fat: Signal drop on fat-saturated T1.
- 7- Microscopic fat: Detected by reversed chemical shift artefact in the in and out phases or DWIs.
- 8- Keratinoid material detected by DWIs (fluid signal with restriction and low ADC values).

The lesion is large predominant solid with cystic areas with higher attenuation fluid density more than 10 HU and intratumoral fat \pm widespread calcification, in 2nd decade of life.

Features which enhance the diagnosis of monodermal struma ovarli teratomas:

Complex cystic/solid masses with cstic areas of variable signal on both T1 & T2. On CT, colloid material demonstrates high attenuation. Following contrast, most tumors exhibit moderate or no enhancement of the cystic wall with positive clinical manifestation and Labs of hyperthyroidism.

Fig. (1): An algorithmic way for easier identification of MCT and its complication.

Statistical analysis and sample size calculation:

The sample size for sensitivity and specificity detection was estimated using the sample size equation (20), using the following parameters: Expected sensitivity 89%, specificity 82%. Disease prevalence 20%, precision \pm 20%, confidence interval 95%, and level of significance 0.05, the sample size was estimated to be study group N=80. The

analysis was conducted using SPSS version 28 statistical software for the social sciences (Armonk, NY, USA: IBM Corp.). While frequencies (number of cases) and relative frequencies (percentages) were used for categorical variables, the mean and standard deviation were used for quantitative variables. Various imaging modalities' sensitivity was computed.

Results

The current study included 80 females who met the previously indicated inclusion and exclusion criteria. Our participants ranged in age from 13 to 50 years old, with a mean age of 34.67±7.15. According to the clinical presentation of our patients; most of our cases (72/80;90%) presented with chronic abdominal and pelvic pain. Five cases were asymptomatic and discovered accidentally. Two cases had acute abdominal pain at the time of their diagnosis, and one case presented with acute urine retention.

After subjecting all our participants of both groups to the US examination; we concluded that most of our cases were unilateral in site (n=68/80 85%) and (n=12/80 15%) had bilateral ovarian lesions. So ninety-two ovarian lesions were included in our study, their maximum diameters ranged from

3.5-10cm with a mean of 15.2±1.16 at the setting of the US study.

Fifty patients exhibited the characteristic features of MCT and were identified with US alone as MCTs with proper pathological association throughout the preoperative phase. When patients (n=30) could not be pre-diagnosed with US due to unusual characteristics or if their tumor markers were elevated (particularly CA-125), computed tomography and magnetic resonance imaging (MRI) were performed as an extra radiological assessment

Based on our US image interpretation of the typical study group participants, the distribution of their findings incidence was displayed in (Table 1). Wide variable imaging interpretations of the atypical group of patients were identified in our study by imaging modalities. The distribution of their findings' incidence was shown in (Table 2).

Table (1): Incidence distribution of US findings of our typical group patients (n=50).

Imaging sign	Incidence	Us interpretation
- Rokitansky nodule (dermoid plug)	30/50 (60%)	- A densely echogenic tubercle projecting into the cystic lumen.
- Tip of the iceberg sign	5/50 (10%)	 A mixture of fatty fluid, hair, and cellular debris create an echogenic focus with acoustic shadowing.
- Dot-dash sign	10/50 (20%)	 Hyperechoic lines and dots of hairs in different orientations within the imaging plane.
- Fat-fluid / fluid-fluid level	6/50 (I1.2%)	 Anechoic sebum layered above hyperechoic aqueous/debris containing debris-containing, the reverse.
- Floating balls sign	1/50 (2%)	 Intracystic floating hyperechoic globules moving with changing the position of the patient.
- Comet tail appearance	3/50 (6%)	- Hypoechoic hairballs with posterior acoustic shadowing.
- Intratumoral fat	4/50 (8%)	- Diffuse or regional high amplitude echoes.
- Tooth/ calcification. Tuft of hair	15/50 (30%)	- Regional high amplitude echoes with shadowing.
- Intratumoral fat	4/50 (8%)	- Diffuse or regional high amplitude echoes.

Table (2): Incidence distribution of our radiological findings among atypical group patients (n=30).

Imaging findings	Incidence
Pure cystic With lesional wall fat. Without fat Pure cystic with scanty fat. Pure fatty lesion	4/30 (13.3%) 3/4 1/4 5/30 (16.6%) 1/30 (3.3%)
 Predominant solid: With few fatty areas Without fat Enhanced solid pattern Non-enhanced solid pattern 	12/30 (40%) 10/12 2/12 2/12 10/12
Complex cystic and solid:Enhanced patternNon-enhanced patternFat	7/30 (23.3%) 1/7 6/7 6/7
Multilocular cystic with intraregional fat	1/30 (3.3%)
DWI Restricted: • Non-solid components • Solid components	10/30 (33.3%) 8/10 2/10
Calcification /tuft of hair	4/30 (13.3%)

According to the postoperative histopathological assessments that were done for our study group patients; seventy-six cases were diagnosed as mature cystic teratomas, two cases presented with col-

lision tumors [teratoma with mucinous cystadenoma (Fig. 2) and teratoma with dysgerminoma (Fig. 3)], one case was Struma ovarii, and one case was an immature teratoma.

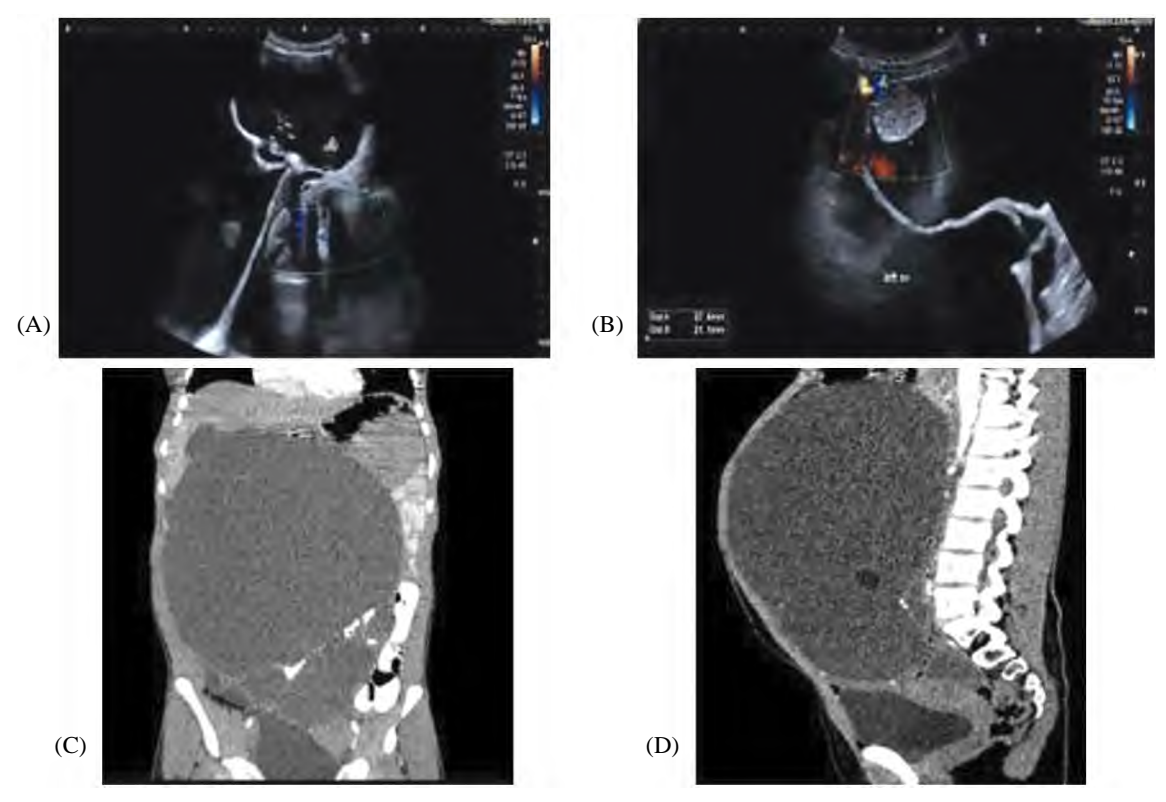


Fig. (2): Female 13 years: Presenting by abdominal pain and distension US with color Doppler A. B: Large multilocular cystic mass filling the abdominal quadrants, a hanging papilla is seen not typically fat density (arrowhead) CT was done C. coronal & D. sagittal reconstruction revealed a large multilocular mass. Lower septae showing calcification, note also a small fat globule seen (arrow). CT picture was suggestive of mature cystic teratoma on top of mucinous tumor. Pathology revealed mature cystic teratoma.

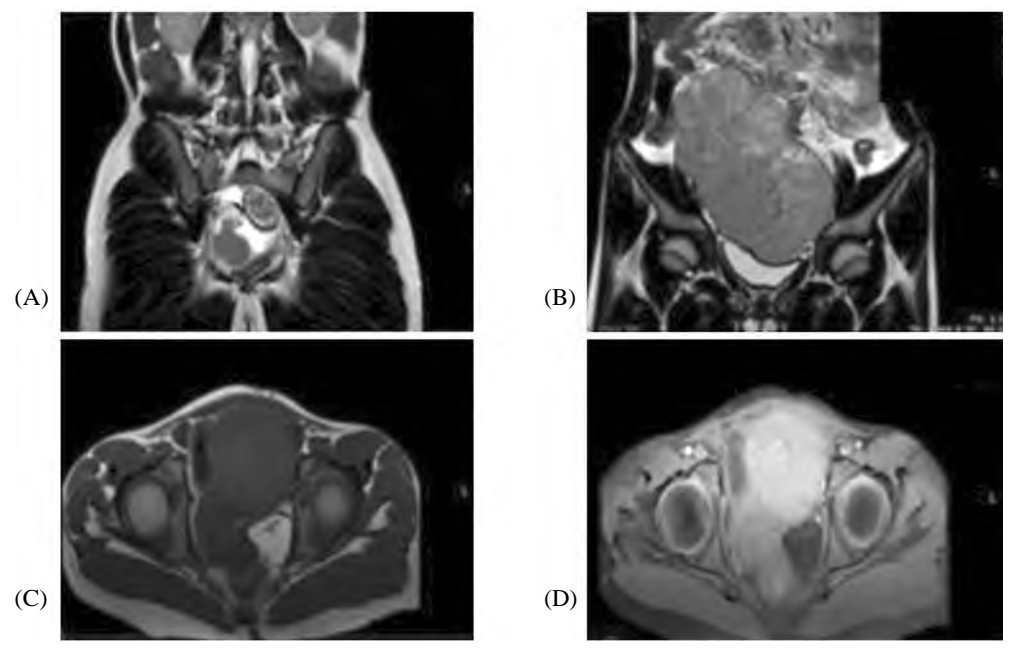


Fig. (3): Female 14 years presenting by abdominal enlargement, MRI was done bilateral solid ovarian tumors A smaller on the right with ovarian peak sign B. large left one C&D T1 & T1 fat suppression revealed another coincident mass with fat signal bright in T1, suppressed on T2. Collision tumor on the left mature cystic teratoma, bilateral dysgerminoma.

With the retrospective revision of imaging, the Struma ovarii case was reported as complex ovarian lesions with variable fluid densities/signal intensities owing to the thick, gelatinous colloid of the struma. Fat and calcification were also identified. Revised laboratory tests; CA 125 was elevated and the patient was euthyroid.

Retrospective analysis and distribution of the available preoperative serum level of the tumor markers are shown in Table (3). Among the avail-

able tumor markers, CA 19-9 revealed the highest elevated rate (23.3%), whereas CEA revealed the lowest (3.8%). Both AFP and B-HCG were elevated in the cases of immature teratoma and the collision tumor of mixed dysgerminoma with teratoma. Only one case showed mild increased serum level of CEA with no underlying malignancy detected on its pathological correlation. Sensitivity of the available tumor markers CA 19-9, CA 125, AFP and B-HCG were respectively calculated to be 23.3%, 15% and 11.1%.

Table (3): Prevalence of serum Tumor markers in our included cases.

Tumor marker	Elevated rate n/total	Serum level range	Mean ± SD	Tumor size
AFP (ng/mL)	4/28 (14.2%)	0.7–19.2	1.9±1.7	3.4-6.3
B-HCG (mIU/mL)	3/27 (11.5%)	5.3-8.1	6.7±1.4	4.2-7
CA 19-9 (U/mL)	14/60 (23.3%)	0.6–985	86.5±180.2	4-10
CA 12 (U/mL)	9/60 (15%)	1.6–220	26.1±28.9	4-10
CEA (ng/ml)	1/26 (3.8%)	4.5		4.8

CA 19-9 elevation was linked to nine aberrant CA 125 in 14 MCT cases. Therefore, in our examined instances, we compared patients with and without a high CA 19-9 level; the results are shown in Table 4. Patients with increased CA 19-9 levels had considerably larger tumors on average $(7.06\pm1.6 \text{ cm vs. } 3.9\pm0.4 \text{ cm, respectively, } p=0.01)$

than those with normal CA 19-9 levels. Similarly, nine patients with increased blood CA 19-9 had significantly higher mean serum CA 125 levels and rates. Of the individuals with normal CA 19-9 levels, only two had increased serum CA 125. Those with elevated serum CA 19-9 showed a significantly higher rate of bilaterality than the other group.

Table (4): Prevalence of serum CA 19-9 in our studied cases.

	Patients with elevated CA 19.9 (N = 14)	Patients with normal CA19.9 (N = 46)	<i>p</i> -value
Age	34.5±14.1	33.9±10.02	0.758
Menopause n (%)	3 (21.4)	9 (19.5)	0.754
Tumor size	7.06 cm±1.6	3.9 cm±0.4	0.01
Bilaterality	10	2	
Serum level CA19.9 (mean ± SD)	86.5±180.2	11.3±8.4	< 0.01
Elevated CA 125 n (%)	9 (64.2%)	2 (4.3%)	< 0.01
Serum CA 125 level (mean ± SD)	26.1±28.9	18±9.3	0.10

The most specific sign for the diagnosis of MCTs was the presence of fat. In the atypical group, twenty-six cases were preliminarily interpreted as MCTs by CT/MRI based on fat recognition. Its distribution was variable; either a scanty amount, diffuse fatty, or lesional wall fat (Fig. 4).

The superiority of MRI over CT in microscopic fat identification by T1 in & out phases was noticed in those cases presented by pure cysts with fat in their wall. Calcification/tuft of hair was detected by CT in four cases of the atypical group which aids in MCTs diagnosis.

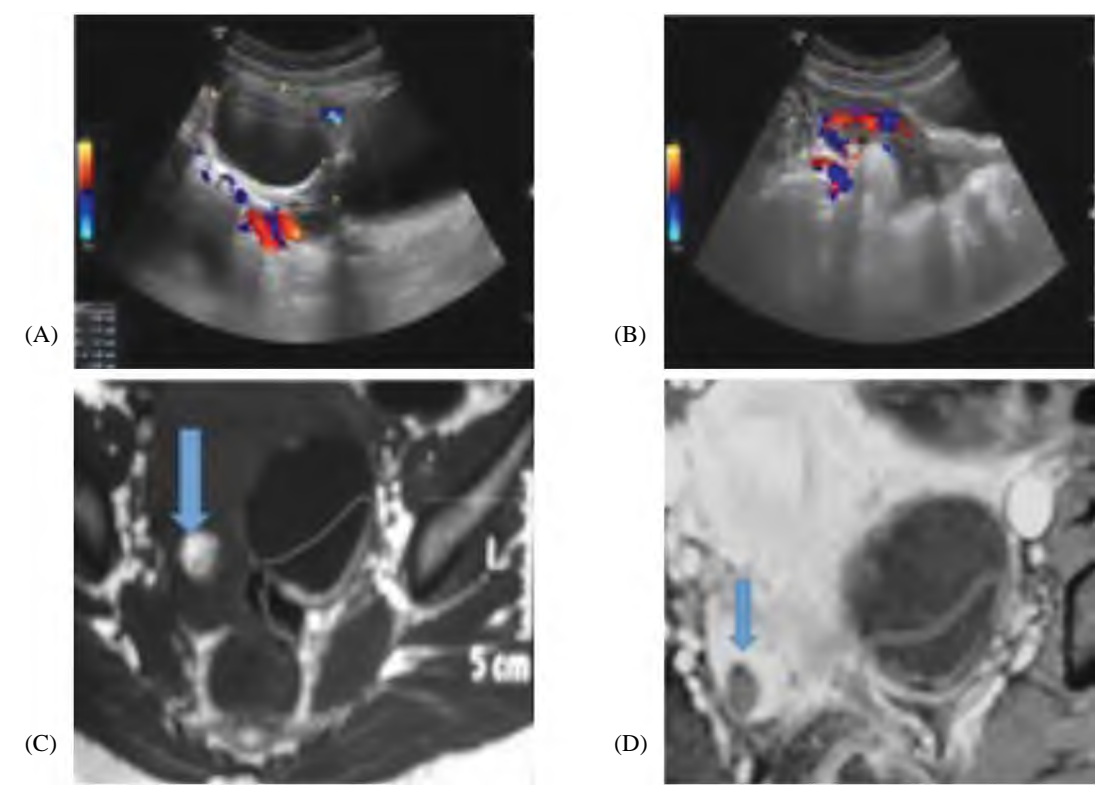


Fig. (4): An accidentally discovered left ovarian cyst A. Ultrasound showed a thick echogenic wall, not vascular on color Doppler B. small echogenic lesion in the right ovary. MRI showing bilateral mature cystic teratomas with different appearances A. Axial T1 showed a bright signal within the right ovarian cyst (arrow), while the left showed a thick bright wall (red circle) B. axial T1 SPIR: Both are suppressed.

DWI alone is misleading as almost ten out of thirty atypical group patients displayed areas/regionrestricted diffusion with low ADC values (lower than the cutoff value of malignancy). With the correlation to conventional MRI, this bright signal was matched to areas of a fluid signal of low T1 & high T2 in five complex ovarian lesions, and one pure ovarian cyst. In comparison to the histopathological results, those cases showed an appreciable amount of keratinoid material. This finding was highlighted in the MCTs diagnosis, especially in the setting of either pure cystic or complex ovarian lesions.

The "floating ball" presentation, which consists of several tiny floating spheres inside a big cyst, is one of the uncommon atypical MCT presentations that can pose a diagnostic problem in our study (Fig. 5). Histologically, the spheres are made up of different amounts of keratin, fibrin, hemosiderin, sebaceous debris, hair, and fat. This result is thought to be pathognomonic of atypical MCT because it has not been documented for other forms of ovarian cancers.

In the setting of an ovarian tumor was primarily solid or heterogeneously complex lesions with fatty regions±calcifications, a diagnosis of mixed germ

cell tumor (collision tumor) should be raised. In our study, two histopathological proven cases presented with collision tumors (teratoma with mucinous cystadenoma and teratoma with bilateral dysgerminoma). CT was successful in the former one by its typical multiloculated ovarian cystic mass with an internal loculi filled with pure fat density. While diagnosis of the latter lesion was successfully performed by the help of MRI which demonstrated as solid multilobulated bilateral ovarian masses with prominent fibrovascular septa, speckled pattern calcifications, and discrete fatty components.

The presence of solid components was always questioned to exclude underlying malignancy. In our study, we had nineteen cases with solid portions; twelve were predominantly solid and the rest were complex lesions. Based on MRI study analysis of their solid components, three of them showed variable enhancement, most of them were of low T2 signals, and four cases displayed restriction with low ADC values. Malignant transformation was considered and expected to contrast uptake, restricted diffusion, intermediate T2 solid, and abnormal tumor marker (CA 125). In correlation to the postoperative histopathology of those cases no underlying detected malignancy.

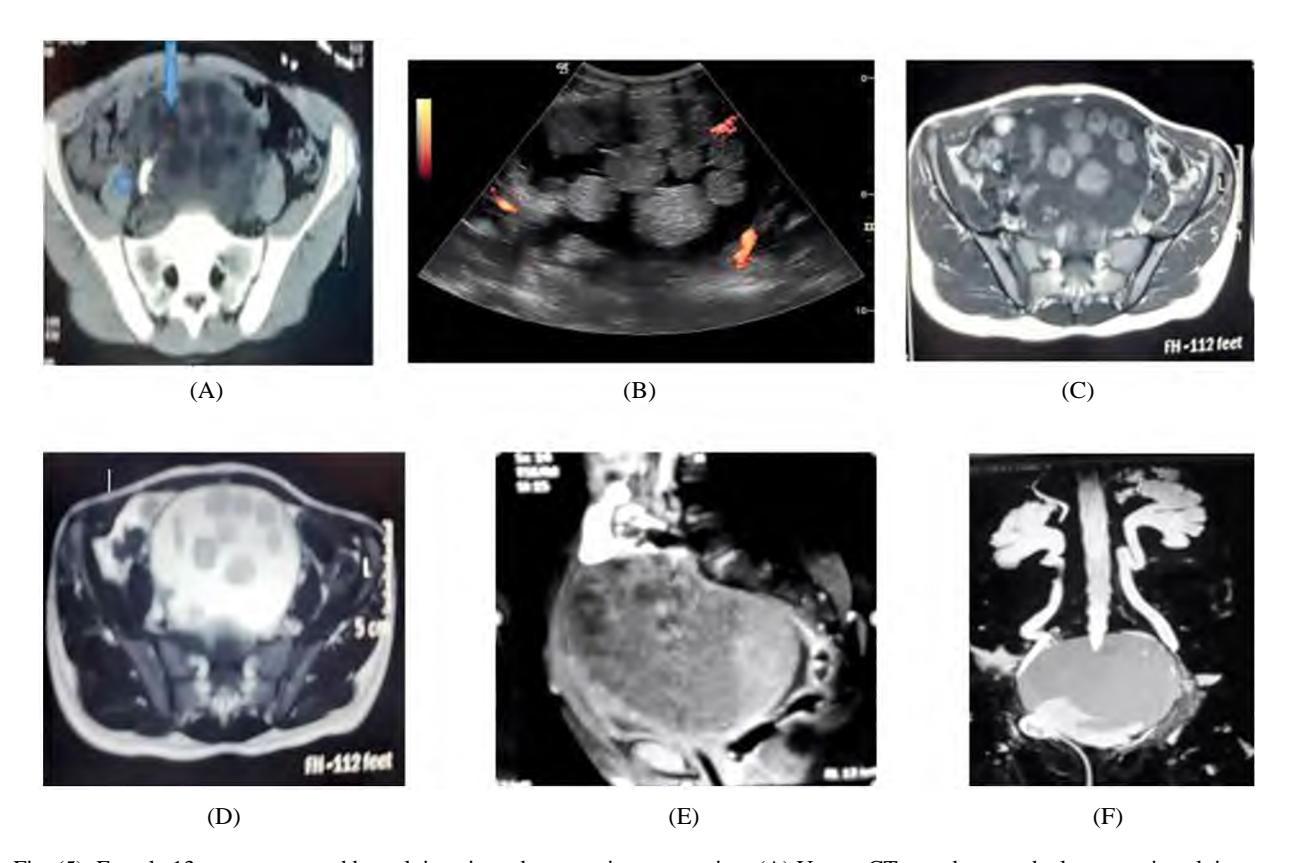


Fig. (5): Female 13 years presented by pelvic pain and acute urinary retention: (A) Urgent CT was done, and a large cystic pelvic mass with a large cystic component contains numerous internal nondependent hypoattenuating spheroid fat globules (blue arrow) and calcific focus (blue arrowhead) is noted. (B) Ultrasound and color Doppler showed nonvascular floating echogenic balls. (C, D&E) Axial T1 and T2 and sagittal T1 fat suppression, the floating balls showed bright signal intensity in the T1- and intermediate T2-weighted sequences, with signal loss in the out-of-phase T1-weighted gradient-echo sequence. (F) MRU showed the cause of urinary retention with the mass incarcerated in the pelvis compressing the bladder with secondary hydroureter, hydronephrosis.

The complication was noticed in two cases presented with acute abdominal pain and preoperatively diagnosed by CT as rupture and torsion with postoperative laparscopic inter-observer agreement of 100%. In our study, the torsed ovary is diagnosed by the Doppler US interpretation of its avascularity, and on its CT examination it revealed; an ovarian mass with cortical follicles, ipsilateral fallopian tube enlargement and thickening, ascites Fig. (6). The ruptured ovarian lesion is diagnosed by voluminous ascites and discontinued distorted wall lesion on both US and CT studies.

With a preoperative sensitivity and specificity of 100% correlated to histopathology, fifty out of eighty cases that underwent ultrasonography were routinely classified as MCTs by their different typical criteria for diagnosis. In the atypical cases, US wasn't conclusive alone, so additional CT and/or

MRI raised our conclusive suggestive diagnosis of teratoma in 26 (86,6%) of total atypical cases based on the presence of fat, bone density, and keratin. Four ovarian lesions were misdiagnosed; two were complex lesions devoid of fat and reported as borderline ovarian lesions, and the other two were predominant solids of low T2 with no restriction interpreted as fibroid.

As a result, our preoperative overall sensitivity for diagnosing unusual cases using these combined modalities was 86.6%. The sensitivity was 80%, and eight out of ten patients in the atypical group who were assessed with CT received an MCT preoperative diagnosis. The preoperative diagnosis of MCTs was corroborated by MRI imaging in 13 out of 15 atypical group individuals, with an 86.6% sensitivity. With 100% sensitivity, five patients were identified as MCTs by both CT and MRI.

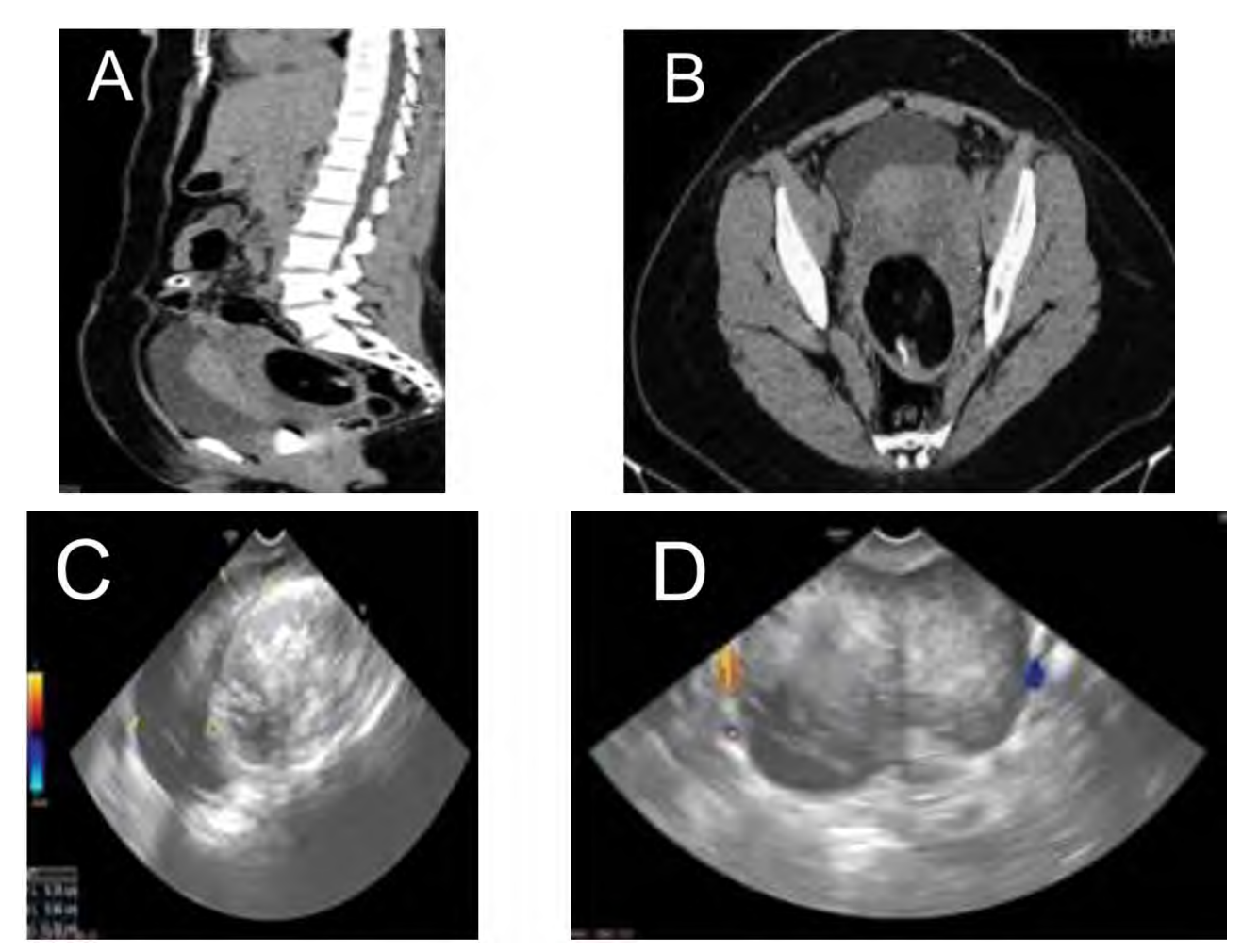


Fig. (6): Female 19 years presenting by acute abdominal pain: Post-contrast CT examination A. Sagittal reconstruction B. Axial cuts showing a large pelvic mass with a fatty component containing mural nodule with calcification and surrounded by unenhanced soft tissue component. look Ultrasound C. Typical appearance of the echogenic cystic component with dot-dash sign D. The surrounding ovary is devoid of vascularity on color Doppler. Ovarian torsion on top of mature cystic teratoma.

Discussion

The most frequent germ cell ovarian tumor is mature cystic teratoma (MCT). It has at least two well-differentiated mature germ cell layers, according to histology (ectoderm, mesoderm, endoderm). MCT is often made comprised of the ectoderm (skin and hair) and mesoderm (fat and muscle) Rha SE et al. [2]. Despite the fact that this tumor is usually asymptomatic and more prevalent during the reproductive phase, it is critical to recognize it early because it can lead to a variety of consequences, including loss of fertility Saglam H et al. [6].

Examples of both common and uncommon MCT imaging representations were shown in this study. Knowing the visual traits of the different kinds of ovarian teratomas can help radiologists make an accurate diagnosis and guide doctors in creating the best treatment plan.

The study's findings indicated that CA 19-9 is superior, and often higher than CA 125 making it more practical marker within MCTs. Our results displayed an increase in CA 19-9 levels up to 23.3% which was similar to Ustunyurt Emin et al that depicted 39.6% of individuals had elevated CA 19-9 levels. This finding highlighted the elevated levels of CA 19-9 in the serum could indicate the presence of MCTs patients with an unknown pelvic mass nature based solely on ultrasound imaging.

Based on previous literature data by Ustunyurt Emin et al. and Dede et al., addressing the association between serum CA 19-9 levels and certain clinical features (size, laterality). We have discussed this issue, and detected significant increase in CA 19-9 levels in bigger tumor size and with higher rate of laterality. This finding was due to the leakage of CA 19-9 into the blood flow was more likely to occur in both situations. Next, another sig-

nificantly heightened CA 19-9 level was a frequent discovery in patients with MCTs, in which it did not require prompt assessment of digestive system.

With a sensitivity of 100 percent, fifty patients were accurately identified as MCT preoperatively using only USG in comparison to both histological and surgical results. Because the majority of these instances (30/50) had the standard imaging features of an ovarian teratoma, a cystic mass with a highly echogenic tubercle (Rokitansky nodule), and intratumoral fat. These results are similar to Saglam H et al. [6] who determined that sensitivity was 67.2% according to findings in USG, and de Kroon et al. found sensitivity to 80% and specificity to 89% in studies involving 99 dermoid cysts.

Saglam H et al. [6] claimed that the levels of fat-liquid, focal or diffuse hyperechoic foci/ridges created by hair, and acoustic shadowing can all be observed at 90%, 60%, and 10%, respectively, as typical characteristics of MCTs. On line with this study, our results depicted those typical imaging abnormalities in thirty-nine patients, with rates of 22%, 36%, 11.2%, and 10% respectively.

Although radiologists are familiar with typical MCT imaging results, unusual imaging aspects can be particularly deceptive. Out of eighty patients in our study, thirty cases weren't conclusive by US alone. Considering the features reported with them; nine (30%) cases were purely cystic, twelve (40%) cases were predominant solid, seven (23.3%) cases were complex cystic with solid, and fat density was detected at 86.6%. These atypical findings were studied by Saglam H et al. [6]. They found that the solid structure was evaluated at 28.1%, the solid-cystic structure at 40%, the fat density at 75%, and the cystic structure at 31.3%.

One of uncommon atypical presentation of MCTs was multiple little floating spheres within a single big ovarian cyst known as the "floating ball." We illustrated one case shown this finding with 2nd ry acute urine retention, hydroureter, and hydrone-phrosis (Fig. 7). Espindola, A. [8] revealed the same case result. According to histology, the spheres are composed of different amounts of keratin, fibrin, hemosiderin, sebaceous debris, hair, and fat. This is believed to be pathognomonic for MCTs because it hasn't been observed in other types of cancers.

Using a gradient-echo approach with both inphase and opposed-phase imaging, it is crucial to thoroughly analyze any fat in the cystic wall when dealing with solely cystic ovarian lesions that show no fat in order to make the proper preoperative diagnosis. This approach is probably superior to the fat saturation method. This finding was highlighted the role of MRI in our atypical four cases of MCTs, and it was also supported by S. Wakrim and M. EL did J [9] who were concerned and presented atypical cases of MCTs in their review article.

DWI had an important role in our study to diagnose MCTs, especially those having no fat and presenting as pure cystic or complex lesions. We agreed with a study by Nakayama et al. [10] who discussed that; DWI and its resultant ADC values clearly separated these two substances, even though keratinoid material radiologically approximated serous fluid. The keratinoid substance's limited Brownian mobility causes a high DWI signal with an ADC value that is even lower than that of cancer. Accordingly, a strict radiologic-pathologic correlation should be taken into consideration for the cystic fatless mature cystic teratoma, and to discriminate it easily from serous ovarian cystic lesions.

CT had been played a crucial role over MRI in easier recognition of intralesional calcification/bone densities. Calcification with very high HU values points to the presence of enamel and a tooth-like structure (higher than bone). In our study nineteen (23.7%) cases out of eighty displayed bone density detected by US and CT. That was near to the study by Saglam H et al. [6] that noted fifteen cases were detected with bone density by CT and MRI.

CT and MRI had been aiding in diagnosis of collision tumors of the ovary in our study. Detection of fat whatever its amount in a predominantly solid/complex ovarian lesion should raise its possibilities. Two cases had been included in our study and was successfully diagnosed in correlation to their histopathological results. Their typical imaging findings were supported by a studies of Park BS et al. [4], Rha et al., and P. Rios et al. [3].

We encountered in this study, one case diagnosed by pathology as immature teratoma, and its US findings weren't conclusive alone but with aid of MRI and CT, it was reported as a large solid lesion with coarse calcification and scanty amount of fat; suggestive of immature teratoma. That was in line with Sabaa L et al. [5] who mentioned, Immature teratomas are commonly present on CT and MR scans. There is frequently a big irregular solid component with coarse calcifications and small fat foci, as well as hemorrhage.

Thirty cases in our study showed atypical features of MCT, therefore additional CT/MRI with

USG was used to enhance our conclusive findings. The sensitivity of those combined modalities was estimated to correctly reach the final diagnosis compared to the histopathological and intraoperative findings in 26 cases out of 30 up to 86.6%. On the other hand, a study by Saglam H et al. [6] included On one hundred and thirteen cases, ultrasonography, computed tomography, and magnetic resonance imaging revealed that one hundred and three were operated on, with the sensitivity of the preoperative screening procedures calculated to be 75.5 percent.

The limitation of this study is the small number of the included atypical cases of MCT. Potential susceptibility artifacts brought on by nearby intestinal gas could have impacted the ADC value or the signal strength on DWI. For these issues to be resolved, technological advancements could be required. We did not entitle the different histological patterns of MCT in our study and correlate them to radiological interpretation as we already had a few cases of different histology. Also, because of the limited cases of the complication, we did not statistically analyze the ADC values discriminating between MCT and its malignant transformation.

Conclusions:

The common and atypical imaging features of teratomas, as well as their consequences, were highlighted. Sonography is still the most used imaging method for determining MCT, and it is diagnostic in most cases. In rare circumstances, further CT, MRI, or both were virtually diagnostic.

References

1- SEIGEL M.R., REBECCA J. WOLSKY2, EDWIN A. AL-VAREZ1, et al.: Struma ovarii with atypical features and synchronous primary thyroid cancer: A case report and review of the literature. Archives of Gynecology and Obstetrics, 300: 1693–1707, 2019.

- 2- SAHIN H., ABDULLAZADE S. and SANCI M.: Mature cystic teratoma of the ovary: A cutting edge overview on imaging features, 8: 227–241, 2017.
- 3- RHA S.E., BYUN J.Y., JUNG S.E., HYO LIM, et al.: Atypical CT and MRI Manifestations of Mature Ovarian Cystic Teratomas, AJR Am. J. Roentgenol., 183: 743-50, 2004.
- 4- PARK B.S., KIM K.J., KIM K.R. and CHO K.S.: Imaging Findings of Complications and Unusual Manifestations of Ovarian Teratomas; RadioGraphics, 28: 969–983, 2008.
- 5- SABAA L., GUERRIEROD S. and SULCIS R.: Mature and immature ovarian teratomas: CT, US and MR imaging characteristics. European Journal of Radiology, 72: 454–463, 2009.
- 6- SAGLAM H., ATALAY F., AVSAR A.F., et al.: The predictive value of the preoperative diagnostic tests in mature cystic teratomas of the ovary. Clin. J. Obstet. Gynecol., 1: 073-081, 2018.
- 7- PENG Y., LIN J., GUAN J., et al.: Ovarian collision tumors: Imaging findings, pathological characteristics, diagnosis, and differential diagnosis. Abdom Radiol., 43: 2156–2168, 2018. https://doi.org/10.1007/s00261-017-1419-6.
- 8- ESPINDOLA A., AMORIM V.B., KOCH H.A., et al.: Atypical presentation of mature cystic teratoma ("floating balls"). Radiologia Brasileira, 50 (3): 206–207, 2017.
- WAKRIM S. and EL J. DID M.: Mature Ovarian Teratoma: Atypical Imaging. Case Rep Radiol., Feb 18; 2020: 1352961, 2020. doi: 10.1155/2020/1352961. PMID: 32148993; PMCID: PMC7053484.
- 10- NAKAYAMA T., YOSHIMITSU K., IRIE H., et al.: Diffusion-weighted echo-planar MR imaging and ADC mapping in the differential diagnosis of ovarian cystic masses: Usefulness of detecting keratinoid substances in mature cystic teratomas. J. Magn. Reson. Imaging, 22: 271-278, 2005. https://doi.org/10.1002/jmri.20369.
- 11- HOSOKAWA T., SATO Y., SEKI T., et al.: Malignant transformation of a mature cystic teratoma of the ovary with rupture; Jpn. J. Radiol., 28: 372–375, 2010.

الخصائص التصويرية للورم المسخي المبيضي النموذجى وغير النموذجى، مراجعة شاملة: الارتباط المرضى الإشعاعى

الورم المسخى هو نوع شائع من أورام المبيض يحدث في الخلايا الجرثومية. يمثل ٢٠٪ من أورام المبيض في البالغين و٥٠ من أورام المبيض في البالغين و٥٠ من أورام المبيض في الأطفال. ينقسم الورم المسخي إلى نوعين رئيسيين: الناضج وغير الناضج. الأورام المسخية الناضجة هي الأكثر شيوعًا وتشكل معظم الحالات. من الصعب التمييز بينها وبين أورام أخرى غير سرطانية. الأورام المسخية غير الناضجة تشكل النوع الثاني الأكثر شيوعًا وهي أكثر خطورة. من المهم فهم المظاهر غير النمطية للأورام المسخية المبيضية لتشخيصها ومعالجتها بشكل صحيح. قد يكون التصوير بالأشعة فوق الصوتية مفيدًا في اكتشاف هذه الأورام وتحديد المظاهر الغير نمطية للمساعدة في تتسين شخيصها. ضرورة التشخيص المبكر والتعامل السليم مع المضاعفات المحتملة للوقوف على التغيرات التي يمكن أن تساهم في تحسين النتائج للمرضى.

يثبت البحث أن التشخيص المبكر للأورام المسخية المبيضية غير النمطية يعزز فرص العلاج الفعّال. بالإضافة، فإن استخدام التصوير المتقدم مثل الأشعة المقطعية والرنين المغناطيسي يمكن أن يساعد في تمييز المظاهر غير النمطية للأورام، ومن الجدير بالذكر أن هذه المظاهر تعتمد على مكوّنات الورم ومضاعفاته. بناءً على ذلك، قد يستفيد الأطباء من تحليل شامل للأورام المسخية المبيضية غير النمطية بهدف توفير التشخيص السليم وتحديد أفضل طريقة علاج. فهم المظاهر غير النمطية للأورام المسخية المبيضية غير النمطية يساهم في تحسين تشخيص ومعالجة المرض. بالنظر إلى أن بعض الأورام المسخية لا تحتوى على دهون وتظهر بشكل مشابه للأورام البطانية الأخرى، يعد الإدراك المبكر لتلك الأورام أمرًا هامًا. من الضروري أيضًا فهم نتائج التصوير لمضاعفات الورم المسخى المبيضى، حيث أن التشخيص الدقيق والفورى لتلك المضاعفات يمكن أن يحسن حالة المرضى ويزيد من فرص العلاج الناجح. لذلك، ليجب على الأطباء العناية الشديدة بتحليل كافة العلامات والمظاهر للأورام المسخية ومضاعفاتها بغية الكشف المبكر والتدخل المناسب.